

# Normal or abnormal isospin-fractionation as a qualitative probe of nuclear symmetry energy at supradensities

Wenmei Guo<sup>1,2,3,4</sup>, Gaochan Yong<sup>1,6,7,\*</sup>, Yongjia Wang<sup>4,5</sup>, Qingfeng Li<sup>4</sup>, Hongfei Zhang<sup>5,6,7</sup>, and Wei Zuo<sup>1,6,7</sup>

<sup>1</sup>*Institute of Modern Physics,*

*Chinese Academy of Sciences, Lanzhou 730000, China*

<sup>2</sup>*School of Physical Science and Technology,  
Lanzhou University, Lanzhou 730000, China*

<sup>3</sup>*University of Chinese Academy of Sciences,  
Beijing 100049, China*

<sup>4</sup>*School of Science, Huzhou University,  
Huzhou 313000, China*

<sup>5</sup>*School of Nuclear Science and Technology,  
Lanzhou University, Lanzhou 730000, China*

<sup>6</sup>*State Key Laboratory of Theoretical Physics,  
Institute of Theoretical Physics,*

*Chinese Academy of Sciences, Beijing, 100190*

<sup>7</sup>*Kavli Institute for Theoretical Physics,  
Chinese Academy of Sciences, Beijing 100190, China*

(Dated: October 8, 2014)

Within two different frameworks of isospin-dependent transport model, effect of nuclear symmetry energy at supradensities on the isospin-fractionation (IsoF) was investigated. With positive/negative symmetry potential at supradensities (i.e., values of symmetry energy increase/decrease with density above saturation density), for energetic nucleons, the value of neutron to proton ratio of free nucleons is larger/smaller than that of bound nucleon fragments. Compared with extensively studied quantitative observables of nuclear symmetry energy, the normal or abnormal isospin-fractionation of energetic nucleons can be a qualitative probe of nuclear symmetry energy at supradensities.

PACS numbers: 25.70.-z, 21.65.Mn, 21.65.Ef

The symmetry energy, which governs phenomena from the structure of exotic nuclei to astrophysical processes, has many ramifications in both nuclear physics and astrophysics [1–4] and also the study of Gravitational waves [5]. Unfortunately, nowadays predictions on nuclear symmetry energy especially at supra-saturation densities are significantly different for different many-body theory approaches [6].

Although nuclear symmetry energy and its slope at normal density of nuclear matter from recent 28 analyses of terrestrial nuclear laboratory experiments and astrophysical observations have been roughly pinned down [7], recent interpretations of FOPI [8] and FOPI-LAND [9, 10] data by different transport models give divergent density-dependent symmetry energy at supradensities [9–13]. Divergence is shown in figure 1. One sees that the constraints from elliptic flow obtained by using different models (UrQMD and Tübingen QMD, as well as the newly updated version of UrQMD model, see refs. [9, 10, 31]) are quite consistent among them, whereas the three constraints from  $\pi^-/\pi^+$  diverges [11–13]. In fact the use of  $\pi^-/\pi^+$  ratio to constraint nuclear symmetry energy raises several doubts: Pion has large freeze-out time, delta and pion scattering and re-absorption may

destroy the high density signals [14]. Treatment of delta dynamics and isospin-dependent pion in-medium effects in transport models is not so straightforward [15–17]. Recent work of MSU groups demonstrates that the ratio of pions spectra is more sensitive than ratios of integrated yields [18]. However, they did not distinguish pions messenger of high density from the rest [19]. Moreover the super-soft behavior of Xie *et al* [13] and Xiao *et al* [11] is not fairly compatible with neutron star stability and structure except introducing non-Newtonian gravity [20].

Putting  $\pi^-/\pi^+$  ratio aside, based on two different transport models we propose isospin-fractionation of energetic nucleons and fragments as a qualitative probe of nuclear symmetry energy in heavy-ion collision at intermediate energies. We find that with very soft symmetry energy, abnormal isospin-fractionation in heavy-ion collision at intermediate energies occurs, whereas with the stiff symmetry energy normal isospin-fractionation is obtained. If having kinetic energy distribution of free and bound nucleons data from, e.g, central Au+Au reaction at 400 MeV/nucleon (as done by FOPI-LAND Collaboration [9, 10]), then one can qualitatively determine high-density behavior of nuclear symmetry energy.

In our used IBUU04 model, besides isospin-dependent initialization and pauli-blocking, an isospin- and momentum-dependent mean-field potential is adopted,

---

\*Electronic address: yonggaochan@impcas.ac.cn

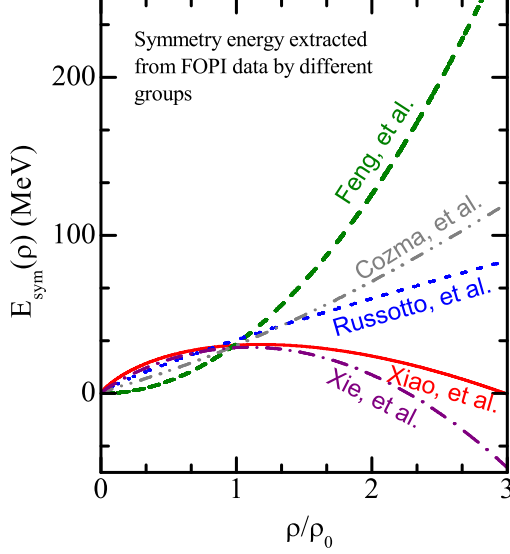


FIG. 1: Density dependent nuclear symmetry energy extracted from FOPI and FOPI-LAND data by different groups. Xiao *et al.* made IBUU04 calculations and compared with FOPI pion data [11]. Feng *et al.* made LQMD calculations and also compared with FOPI pion data [12]. Russotto *et al.* made UrQMD calculations and compared with FOPI-LAND nucleon elliptic flow data [9]. Xie *et al.* made Boltzmann-Langevin model calculations and compared with FOPI pion data [13]. Cozma *et al.* made Tübingen quantum molecular dynamics (QMD) model calculations and compared with FOPI-LAND elliptic flow data [10].

i.e.,

$$\begin{aligned}
 U(\rho, \delta, \mathbf{p}, \tau) = & A_u(x) \frac{\rho_{\tau'}}{\rho_0} + A_l(x) \frac{\rho_{\tau}}{\rho_0} \\
 & + B \left( \frac{\rho}{\rho_0} \right)^{\sigma} (1 - x \delta^2) - 8x\tau \frac{B}{\sigma + 1} \frac{\rho^{\sigma-1}}{\rho_0^{\sigma}} \delta \rho_{\tau'} \\
 & + \frac{2C_{\tau, \tau}}{\rho_0} \int d^3 \mathbf{p}' \frac{f_{\tau}(\mathbf{r}, \mathbf{p}')}{1 + (\mathbf{p} - \mathbf{p}')^2 / \Lambda^2} \\
 & + \frac{2C_{\tau, \tau'}}{\rho_0} \int d^3 \mathbf{p}' \frac{f_{\tau'}(\mathbf{r}, \mathbf{p}')}{1 + (\mathbf{p} - \mathbf{p}')^2 / \Lambda^2}, \quad (1)
 \end{aligned}$$

where  $\delta = (\rho_n - \rho_p) / (\rho_n + \rho_p)$  is the isospin asymmetry, and  $\rho_n, \rho_p$  are the neutron ( $\tau = 1/2$ ) and the proton ( $\tau = -1/2$ ) densities, respectively, and  $\tau \neq \tau', \sigma = 4/3$ ,  $f_{\tau}(\mathbf{r}, \mathbf{p})$  is the phase-space distribution function at coordinate  $\mathbf{r}$  and momentum  $\mathbf{p}$ . The variable  $x$  is used to mimic different forms of the symmetry energy/potential. More details can be found in the recent paper [21]. In fact within transport model, the kinetic part of the symmetry energy is simulated by using different Fermi momenta for neutrons and protons according to the local Thomas-Fermi approximation while the potential part is taken

into account by using the symmetry potential. Uncertainty of symmetry energy at supradensities thus comes from the model-dependent symmetry potential. Shown in Fig. 2 is nuclear symmetry potential/symmetry energy used in the transport models (together with symmetry potential/symmetry energy used in the UrQMD model). In the IBUU04 model, we employed parameters  $x = -1.2$  and  $x = 1$  to represent the positive and the negative symmetry potentials at supradensities, respectively.

In our used isospin-dependent UrQMD transport model, the potential is expressed as [22]

$$\begin{aligned}
 U = & U_{Sky}^{(2)} + U_{Sky}^{(3)} + U_{Yuk} + U_{Coul} \\
 & + U_{Pau} + U_{md} + U_{sym}. \quad (2)
 \end{aligned}$$

The symmetry potential energy density used in the UrQMD transport model is

$$W_{sym} = (S_0 - \frac{\epsilon_F}{3}) \rho \cdot F(u) \cdot \delta^2, \quad (3)$$

here  $S_0 = 32$  MeV is the symmetry energy at the normal nuclear density  $\rho_0$ .  $\epsilon_F$  is the Fermi kinetic energy at normal nuclear density.  $u = \rho / \rho_0$  is the reduced nuclear density, and  $\delta = (\rho_n - \rho_p) / (\rho_n + \rho_p)$  is isospin asymmetry. The symmetry potential is given by  $U_{sym}^{n(p)} = \partial W_{sym} / \partial \rho_{n(p)}$ . For the density dependent part  $F(u)$ , we use two forms [23]:

$$F(u) = \begin{cases} F_1 = u^{\gamma} & , \quad \gamma > 0 \\ F_2 = u^{\frac{a-u}{a-1}} & , \quad a > 1 \end{cases}. \quad (4)$$

Here parameters  $\gamma$  and  $a$  are used to describe the density dependence of symmetry potential. In figure 2, we choose  $\gamma = 1.5$  and  $a = 1.6$  to describe positive and negative symmetry potentials at supradensities, respectively. We thus adopted roughly consistent forms for the positive or negative symmetry potentials in the used two transport models. As for the two-body scattering cross sections in medium, we used the same in-medium corrected forms as those in Ref. [21].

The isospin-fractionation (IsoF) during nuclear liquid-gas phase transition in dilute asymmetric nuclear matter has been studied extensively [24–27]. It is a common phenomenon that gas phase is more neutron-rich than liquid phase in dilute asymmetric nuclear matter [3, 25, 28]. Here we theoretically confirmed an abnormal phenomenon that the neutron to proton ratio of gas phase becomes smaller than that of liquid phase for energetic nucleons under the action of negative symmetry potential at supradensities.

With positive and negative symmetry potentials at supradensities in the used IBUU04 transport model, we first use a simple local density method to study gas-liquid phase transition. Nucleons with local density less or equal than  $\rho_0/10$  are considered as nuclear gas, with local density larger than  $\rho_0/10$  are considered as nuclear liquid. Shown in Fig. 3 is evolution of n/p ratios of nucleons with local density smaller than  $\rho_0/10$  and larger than  $\rho_0/10$

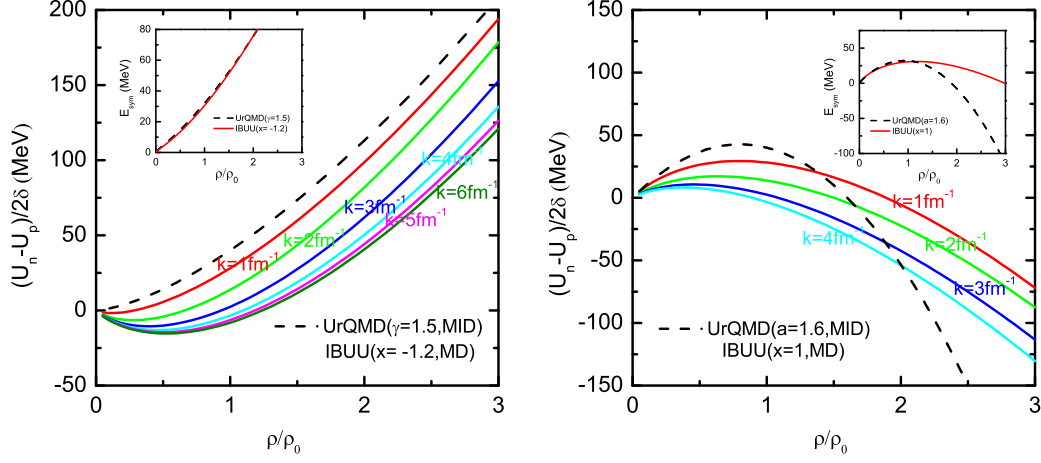


FIG. 2: Density dependent nuclear symmetry potential used in IBUU04 and isospin-dependent UrQMD models. The lines labelled by different momenta (MD) are symmetry potentials used in the IBUU04 model. Symmetry potentials used in present UrQMD model is momentum independent (MID). Left window shows positive potential while Right window shows negative potential, which respectively correspond stiff and soft nuclear symmetry energies at supra-saturation densities.

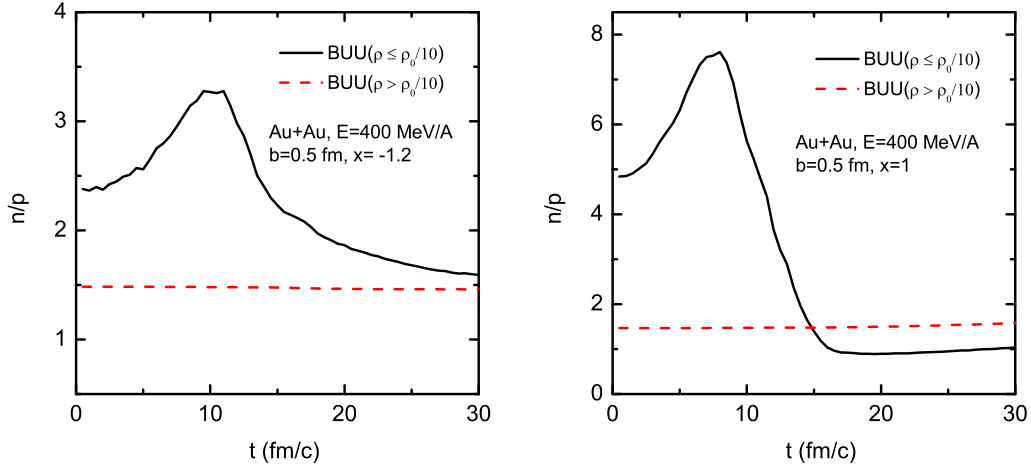


FIG. 3: Evolution of neutron to proton ratio of free and bound nucleons in the central  $^{197}\text{Au} + ^{197}\text{Au}$  reaction at a beam energy of 400 MeV/A with positive (left) and negative (right) symmetry potentials at supra-saturation densities. Simulated with the IBUU04 transport model ( $t_{max} = 40$  fm/c).

from the central  $^{197}\text{Au} + ^{197}\text{Au}$  reaction at a beam energy of 400 MeV/A under the action of positive and negative symmetry potentials at supra-saturation densities. We can see that the  $n/p$  ratio of gas phase ( $\rho \leq \rho_0/10$ ) is larger than that of liquid phase ( $\rho > \rho_0/10$ ) for the positive symmetry potential at supradensities. However, for the negative symmetry potential at supradensities, an opposite conclusion is obtained. The reason is that the negative symmetry potential trends to attractive for neutrons and repulsive for protons during IsoF. Whereas for the positive symmetry potential, neutrons tend to be-

ing repelled by the symmetry potential and protons tend to being attracted during IsoF. Thus we get normal and abnormal gas-liquid phase transition with positive and negative symmetry potentials as shown in Fig. 3.

In real nuclear experiments, one in fact gets free or bound nucleons at final stage. We thus make more realistic predictions on gas-liquid phase transition, i.e., consider  $A = 1$  free nucleons as nuclear gas whereas  $A > 1$  bound nucleons fragments as nuclear liquid. For the IBUU04 model, we give free and bound nucleons fragments analysis as that in Ref. [29]. Figure 4 shows

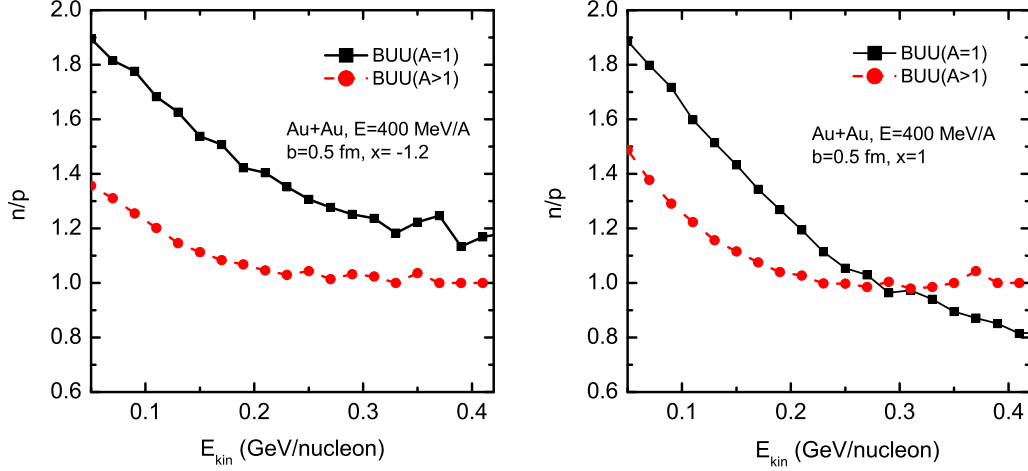


FIG. 4: Neutron to proton ratio  $n/p$  of free and bound nucleons as a function of nucleon kinetic energy in the central  $^{197}\text{Au} + ^{197}\text{Au}$  reaction at a beam energy of 400 MeV/A with positive (left) and negative (right) symmetry potentials at supra-saturation densities. Simulated with the IBUU04 transport model ( $t_{max} = 40$  fm/c).

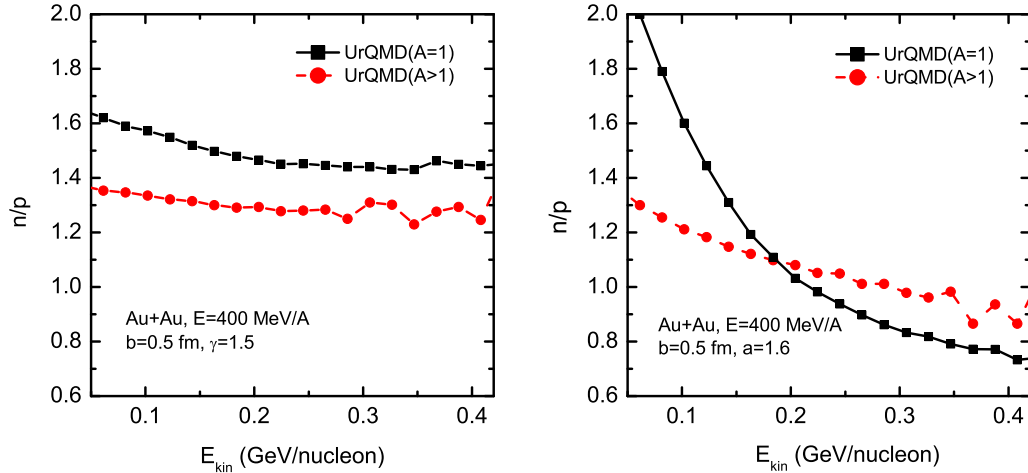


FIG. 5: Neutron to proton ratio  $n/p$  of free and bound nucleons as a function of nucleon kinetic energy in the central  $^{197}\text{Au} + ^{197}\text{Au}$  reaction at a beam energy of 400 MeV/A with positive (left) and negative (right) symmetry potentials at supra-saturation densities. Simulated with the UrQMD transport model ( $t_{max} = 100$  fm/c).

nucleon kinetic energy dependence of the  $n/p$  ratios of free (gas) and bound (liquid) nucleons in the central  $^{197}\text{Au} + ^{197}\text{Au}$  reaction at a beam energy of 400 MeV/A with positive ( $x = -1.2$ ) and negative ( $x = 1$ ) symmetry potentials at supra-saturation densities simulated by the IBUU04 transport model. From the left panel, we can see that the value of  $n/p$  of nuclear gas phase ( $A = 1$ ) is larger than that of liquid phase ( $A > 1$ ) in the whole kinetic energy distribution region with the positive symmetry potential ( $x = -1.2$ ). However, it is interesting to find that the value of  $n/p$  of gas phase ( $A = 1$ ) is smaller

than that of liquid phase ( $A > 1$ ) at higher kinetic energies with the negative symmetry potential ( $x = 1$ ) at supradensities. This phenomenon in fact can be analyzed and checked by FOPI-LAND Collaboration [9, 10].

To further confirm normal and abnormal IsoF at higher energies as previously shown in figure 4, we used the UrQMD (QMD-like model has advantage over many-body correlation and thus frequently used to predict cluster production in heavy-ion collisions [30]) transport model do the same thing, which is shown in Fig. 5. Again the same phenomenon occurs, i.e., at higher kinetic en-

ergy region, the value of  $n/p$  ratio of gas phase ( $A = 1$ ) is becoming smaller than that of liquid phase ( $A > 1$ ) with the negative symmetry potential at supradensities. One discrepancy is that the kinetic energy of transition point with the UrQMD model is lower than that with the IBUU04 model. In fact, the kinetic energy of transition point with the UrQMD model is somewhat  $a$  parameter (shown in Eq. (4)) dependent, but not sensitive to  $a$  parameter. To check the reliability of UrQMD model's predictions, we made the same simulation but switching off symmetry potential. As expected, without symmetry potential the values of  $n/p$  ratio of gas phase ( $A = 1$ ) is almost the same as that of liquid phase ( $A > 1$ ).

Comparing figure 4 with figure 5, with negative symmetry potential at supradensities, why at low energy region both IBUU04 and UrQMD give normal IsoF while at energetic region both show abnormal IsoF? This is because emitted nucleons with lower energies mainly come from low-density region of compressed nuclear matter whereas nucleons with higher energies mainly come from high-density region of compressed nuclear matter, which are mainly affected by low-density and high-density behaviors of nuclear symmetry potential, respectively. As shown in the right panel of figure 2, at low density region the value of symmetry potential is in fact positive whereas at high density region it becomes negative. It is the high-density behavior of nuclear symmetry potential who affects energetic nucleon emission during IsoF.

Therefore energetic nucleon emission reflects high-density behavior of nuclear symmetry energy. The big advantage of using this probe is that one just needs to qualitatively confirm normal or abnormal isospin-fractionation of energetic nucleons experimentally. Compared with other widely studied probes in the literature, this confirmation in fact does not depend on specific numerical values of simulation.

In summary, we provide a qualitative observable, i.e., Iso-fractionation for energies nucleons, to give qualitative determination on nuclear symmetry energy at supra-saturation densities. With positive/negative symmetry potential (i.e., stiff/soft symmetry energy) at supradensities, transport models give normal/abnormal iso-fractionation for energetic nucleons. Future accurate experimental measurements (as done by FOPI-LAND Collaboration) can qualitatively pin down high-density behavior of nuclear symmetry energy by normal or abnormal Iso-fractionation of energetic nucleons.

This work is supported by the National Natural Science Foundation of China (Grant Nos. 11375239, 11435014, 11375062, 11175219, 11175074), the 973 Program of China (No. 2007CB815004), the Knowledge Innovation Project(KJCX2-EW-N01) of Chinese Academy of Sciences, the project sponsored by SRF for ROCS, SEM and the National Key Basic Research Program of China (No. 2013CB834400).

- 
- [1] J.M. Lattimer, M. Prakash, Science **304**, 536 (2004).
  - [2] A.W. Steiner, M. Prakash, J.M. Lattimer, et al., Phys. Rep. **411**, 325 (2005).
  - [3] V. Baran, M. Colonna, V. Greco, M. Di Toro, Phys. Rep. **410**, 335 (2005).
  - [4] B.A. Li, L.W. Chen, and C.M. Ko, Phys. Rep. **464**, 113 (2008).
  - [5] F.J. Fattoyev, W.G. Newton, and B.A. Li, Eur. Phys. J. **A50**, 45 (2014).
  - [6] A.E.L. Dieperink, Y. Dewulf, D. Van Neck, M. Waroquier, and V. Rodin, Phys. Rev. C **68**, 064307 (2003).
  - [7] B.A. Li, X. Han, Phys. Lett. B **727**, 276 (2013).
  - [8] W. Reisdorf, et al., Nucl. Phys. **A848**, 366 (2010).
  - [9] P. Russotto, P.Z. Wu, M. Zoric, M. Chartier, Y. Leifels, R.C. Lemmon, Q. Li, J. Lukasik, A. Pagano, P. Pawłowski, W. Trautmann, Phys. Lett. B **697**, 471 (2011).
  - [10] M.D. Cozma, Y. Leifels and W. Trautmann, Q. Li, P. Russotto, Phys. Rev. C **88**, 044912 (2013).
  - [11] Z.G. Xiao, B.A. Li, L.W. Chen, G.C. Yong, M. Zhang, Phys. Rev. Lett. **102**, 062502 (2009).
  - [12] Z.Q. Feng, G.M. Jin, Phys. Lett. B **683**, 140 (2010).
  - [13] W.J. Xie, J. Su, L. Zhu, F.S. Zhang, Phys. Lett. B **718**, 1510 (2013).
  - [14] G. Ferini, T. Gaitanos, M. Colonna, M. Di Toro, H.H. Wolter, Phys. Rev. Lett. **97**, 202301 (2006).
  - [15] J. Xu, C.M. Ko, Y. Oh, Phys. Rev. C **81**, 024910 (2010).
  - [16] J. Xu, L.W. Chen, C.M. Ko, B.A. Li, Y.G. Ma, Phys. Rev. C **87**, 067601 (2013).
  - [17] T. Song, C.M. Ko, arXiv:1403.7363 (2014).
  - [18] see <https://indico.gsi.de/getFile.py/access?contribId=48&res>
  - [19] H.L. Liu, G.C. Yong, D.H. Wen, arXiv:1406.6504 (2014).
  - [20] D.H. Wen, B.A. Li, L.W. Chen, Phys. Rev. Lett. **103**, 211102 (2009).
  - [21] W.M. Guo, G.C. Yong, Y.J. Wang, Q. Li, H.F. Zhang, W. Zuo, Phys. Lett. B **726**, 211 (2013).
  - [22] Q.F. Li, C.W. Shen, C.C. Guo, Y.J. Wang, Z.X. Li, J. Lukasik, and W. Trautmann, Phys. Rev. C **83**, 044617 (2011).
  - [23] Qingfeng Li, Zhuxia Li, Sven Soff, Marcus Bleicher, and Horst Stöcker, Phys. Rev. C **72**, 034613 (2005).
  - [24] H. Müller and B. D. Serot, Phys. Rev. C **52**, 2072 (1995).
  - [25] B.A. Li, Phys. Rev. Lett. **85**, 4221 (2000).
  - [26] B.A. Li, L.W. Chen, H.R. Ma, J. Xu, G.C. Yong, Phys. Rev. C **76**, 051601 (2007).
  - [27] G.C. Yong, Phys. Rev. C **81**, 054603 (2010).
  - [28] Ph. Chomaz, M. Colonna, J. Randrup, Phys. Rep. **389**, 263 (2004).
  - [29] G.C. Yong, B.A. Li, L. W. Chen, X. C. Zhang, Phys. Rev. C **80**, 044608 (2009).
  - [30] Q.F. Li, Modern Phys. Lett. A **24**, 1, 41 (2009).
  - [31] Y.J. Wang, C.C. Guo, Q.F. Li, H.F. Zhang, Z.X. Li, Y. Leifels, and W. Trautmann, Phys. Rev. C **89**, 044603 (2014).